ACS Catalysis

Research Article

pubs.acs.org/acscatalysis

Photocatalytic Dehalogenation of Vicinal Dibromo Compounds Utilizing Sexithiophene and Visible-Light Irradiation

Christopher D. McTiernan, Spencer P. Pitre, and Juan C. Scaiano*

Department of Chemistry and Centre for Catalysis Research and Innovation, University of Ottawa, 10 Marie Curie, Ottawa, Ontario K1N 6N5, Canada

Supporting Information

ABSTRACT: The reductive dehalogenation of a variety of vicinal-dibromide compounds has been accomplished through the use of α-sexithiophene as an organophotocatalyst. This photocatalytic system brings about the desired transformations in good yields, using low catalyst loadings and short reaction times. To help shed light on the efficiency of this process, we have studied the kinetics of the key mechanistic steps utilizing a combination of steady-state/time-resolved fluorescence and laser flash photolysis techniques.

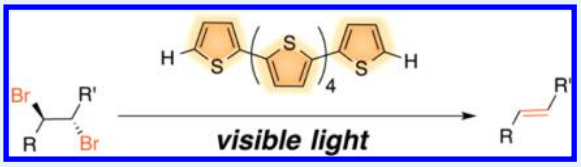

KEYWORDS: *photoredox, metal-free, dehalogenation, kinetics, laser flash photolysis*

INTRODUCTION

The protection and deprotection of olefinic functionalities through bromination and subsequent debromination can be a valuable tool in multistep organic synthesis.[1] Primarily, the protection of these groups as dibromides has a tendency to be simple, straightforward, and, in most cases, high yielding. However, the same cannot always be said of the deprotection process. Until recent developments, in many cases, the most common route to dehalogenation involved the use of highly toxic reductants, such as Zn, Fe, or organotin compounds, which, because of their strongly reducing nature, also suffer from selectivity issues and an incompatibility with a variety of functional groups.[2−5]

To overcome some of these disadvantages, several milder and selective electrocatalytic and photocatalytic reduction systems have been developed to convert vicinal dibromides (*vic*-Br_2) to their corresponding alkenes with enhanced spatial and temporal control.[6−10] For the most part, the electrocatalytic systems have focused on direct two-electron electrochemical reduction; however, the reduction can also be done indirectly through the electrochemical generation of reducing anion radicals or reduced metalloporphyrins.[11,12] The main advantage of the indirect systems being that the desired transformations can be brought about with less energy input, because of the lower overpotentials required.

Similar transformations can be also be accomplished through the use of high-energy ultraviolet (UV) light; however, problems with substrate and product degradation, as well as the need for expensive quartz glassware, have a tendency to make this route impractical.[13,14] For this reason, the photocatalytic systems developed thus far for the dehalogenation of *vic*-Br_2 have focused primarily on the use of visible light (400−700 nm) absorbing transition-metal photocatalysts, such as $Ru(bpy)_3Cl_2$.

Although it has been over 20 years since it was first reported that a system comprising $Ru(bpy)_3Cl_2$ as a photosensitizer and triethylamine as a sacrificial electron donor could be used to reductively dehalogenate *vic*-Br_2 compounds to their corresponding alkenes, there still remains considerable interest in this topic.[7] However, even with such interest, to the best of our knowledge, there is yet to be a metal-free photocatalytic system developed for the reductive dehalogenation of *vic*-Br_2.

Recently, it has been shown that transition-metal photocatalysts can be replaced with less-expensive and less-toxic organic dyes, which, in some cases, actually outcompete their transition-metal counterparts.[15−17] With this in mind, we set out to develop a novel metal-free photocatalytic system for the reductive dehalogenatation of *vic*-Br_2. Drawing inspiration from recent work published by McCulla and co-workers on the visible-light-promoted pinacol coupling of aryl aldehydes utilizing poly(*p*)-phenylene as photocatalyst, we have decided to test the applicability of conjugated oligothiophenes, in particular, α-sexithiophene (α-6T), as a photoredox catalyst.[18,19]

α-6T is an oligomer consisting of six repeating thiophene units. Displaying properties representative of both oligothiophenes and organic semiconductors, it is most commonly employed as an electron donor in organic photovoltaics (OPVs).[20] In addition, it is also well-documented that excited-state oligothiophenes are quite proficient reducing agents, which have been shown to reduce common electron acceptors such as methyl viologen (MV^{2+}),[21] tetracyanoethylene, and C60.[22] It is with this propensity for excited-state electron transfer (eT) that we aimed to develop a photocatalytic system for the dehalogenation of *vic*-Br_2 based on the use of α-6T as a visible-light photoredox catalyst and a tertiary amine as a sacrificial electron donor (see Scheme 1).

Received: July 18, 2014
Revised: September 27, 2014
Published: September 29, 2014

   dx.doi.org/10.1021/cs501030f | ACS Catal. 2014, 4, 4034−4039

Scheme 1. Proposed Mechanism for the Photocatalyzed Reductive Dehalogenation

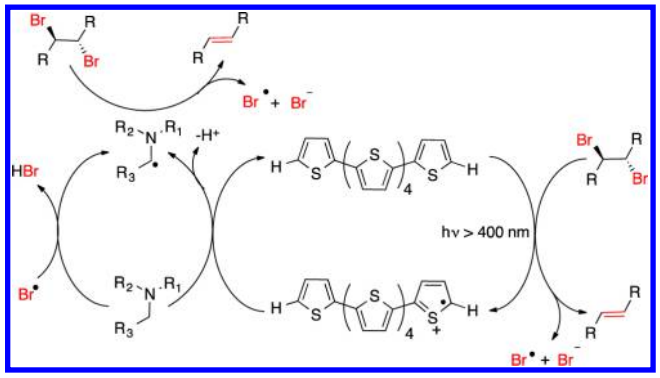

We present here our recent findings on the reductive debromination of a variety of different *vic*-Br_2 compounds utilizing a combination of α-6T, tetramethylenediamine (TMEDA), and visible-light irradiation. To help shed light on the efficiency of this process, we have studied the kinetics of the key mechanistic steps utilizing a combination of steady-state/time-resolved fluorescence and laser flash photolysis techniques.

RESULTS AND DISCUSSION

We began our studies on the reductive dehalogenation of *vic*-Br_2, utilizing α-6T as the photocatalyst, TMEDA as the sacrificial e^- donor, and *meso*-1,2-dibromo-1,2-diphenylethane as our model substrate. In an attempt to optimize the reaction conditions for the dehalogenation reaction, we performed the test reaction under a variety of conditions (see Table 1).

Table 1. Optimization of Reaction Conditions[a]

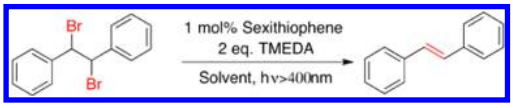

entry/ conditions	TMEDA (equiv)	solvent	atmosphere	time	isolated yield (%)
1 (light)	2	CH_3OH	argon	30 min	N.R.
2 (light)	2	CH_3CN	argon	30 min	18
3 (light)	2	DMF	argon	30 min	76
4 (light)	2	DMF	argon	1 h	>99
5 (light)	2	DMF	air	1 h	68
6 (dark)	2	DMF	argon	1 h	trace
7 (no amine)		DMF	argon	1 h	trace
8 (no catalyst)	2	DMF	argon	1 h	N.R.

[a]Reaction conditions: substrate (60 mM), TMEDA (120 mM), α-6T (0.01 equiv), solvent (5 mL). Irradiated with two warm white LEDs. "N.R." signifies no reaction.

From these initial tests, it was found that (i) the optimal solvent for the dehalogenation is dimethylformamide (DMF) and (ii) at the concentrations employed, one can obtain near quantitative conversion of the model *vic*-Br_2 after only 1 h of irradiation with two warm white LEDs (see Table 1, entry 4). It is also observed that the reaction proceeds with reduced efficiency in the presence of O_2 (Table 1, entry 5). In addition to this, it is also evident that the photocatalyst, sacrificial amine, and light source are all critical components of the system, because their omission results in little or no conversion of the starting material after 1 h (see Table 1, entries 6–8).

With the optimized conditions in hand, we then set out to test our system on a variety of different *vic*-Br_2 compounds. As illustrated in Table 2, our photocatalytic system is able to

Table 2. Photocatalyzed Reductive Dehalogenation of a Variety of *vic*-Dibromo Compounds[a]

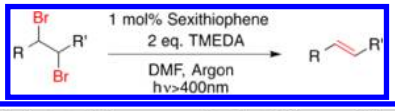

Entry	Substrate (A)	Product (B)	Time	% Yield
1	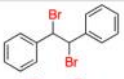	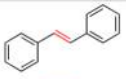	1 h	>99%
2		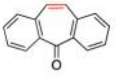	1 h	>99%
3		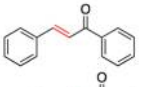	1 h	84%
4		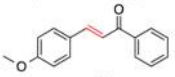	1 h	77%
5		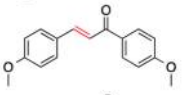	1 h	79%
6		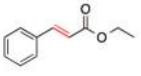	1 h	68%
7			2 h	88%
8		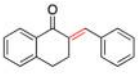	3 h	65%
9	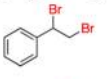		3 h	57%[b]
10		-	3 h	N.R.

[a]Reaction conditions: Substrate (60 mM), TMEDA (120 mM), α-6T (0.01 equiv), DMF (5 mL) under Argon atmosphere. Irradiated with two warm white LEDs. Yields reported as isolated yields. "N.R." signifies no reaction. [b]Percent conversion by ^1H NMR, because of the volatility of styrene.

convert many activated *vic*-Br_2 compounds to their corresponding alkene in good to excellent yields (65%–99%) under short irradiation times (1–3 h). However, as shown by entry 10 in Table 2, our system is unable to reduce the unactivated 1,2-dibromocyclohexane ($E_{1/2}^{red} = -1.40$ V vs SCE),[11] even after 3 h of irradiation, most likely due to the fact that its reduction potential is outside the potential window attainable by the α-6T photocatalyst.

The systems examined are all heterogeneous, since α-6T is barely soluble in organic solvents. It was interesting to establish if we were observing true heterogeneous catalysis, or if the small amount of α-6T that leaches was responsible for the catalysis observed. Experiments in which the supernatant from an α-6T suspension in DMF was tested as a catalyst (see the Supporting Information (SI)) demonstrated that homogeneous catalysis is indeed taking place. In any event, we continued to work with the α-6T suspension, because it offers more experimental convenience and maintains a saturation level of

dx.doi.org/10.1021/cs501030f | ACS Catal. 2014, 4, 4034–4039

catalyst in solution. Detailed experimental results are included in the SI.

At this point, we became interested in examining the mechanism of these reductions in the hope of shedding light onto the origin of the high efficiency exhibited by our photocatalytic system. To accomplish this, we have studied the thermodynamic feasibility and kinetics of the key mechanistic steps outlined in Scheme 1 using *meso*-1,2-dibromo-1,2-diphenylethane as the model substrate. As shown in Scheme 1, the first step in the catalytic cycle upon excitation of α-6T is an excited state electron transfer (eT) from the photocatalyst to the *vic*-Br_2 substrate, which results in the reduction of the *vic*-Br_2 and oxidation of α-6T, leading to the formation of its radical cation (α-$6T^{+\bullet}$). To demonstrate that, indeed, the excited state eT between the catalyst and the model *vic*-Br_2 is thermodynamically feasible, we can calculate the Gibbs free energy for eT from both the singlet and triplet excited state of the photocatalyst, using eq 1.[23]

$$\Delta G_{eT} = E^{ox}_{1/2}(D) - E^{red}_{1/2}(A) - E^{*}_{S\,or\,T}(D) + \Delta E_{Coulombic} \quad (1)$$

The results of the calculation for both the singlet and triplet states of α-6T are shown in Table 3. These values indicate that

Table 3. Thermodynamic Data for Electron Transfer from Excited α-Sexithiophene to the Model *vic*-Br_2 Compound

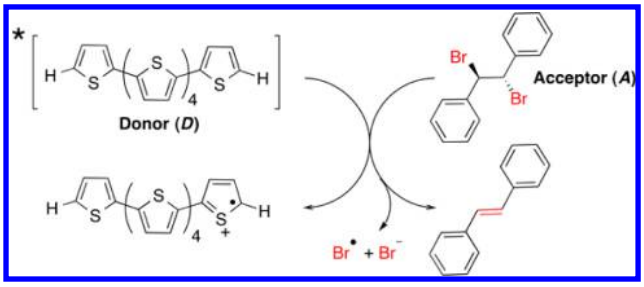

		Thermodynamic Data (kcal mol^{-1})			
entry	excited state	E^*	$E^{ox}_{1/2}(D)^a$	$E^{red}_{1/2}(A)^b$	ΔG_{eT}
1	singlet	59	10	−25	−24
2	triplet	42			−7

[a]Oxidation potential of ground-state donor *D* (α-6T) = 0.415 V vs SCE.[24] [b]Reduction potential of ground-state acceptor *A* (*vic*-Br_2) = −1.10 V vs SCE.[11]

eT from both the singlet and triplet state of α-6T is exergonic. However, because of its higher excited state energy, eT from the singlet is more favorable (by 17 kcal/mol).

While the eT between $^1\alpha$-6T and *vic*-Br_2 is significantly more exothermic than that from the triplet state, given the short lifetime of the singlet (τ_0 = 0.81 ns, see the SI), compared to that of the triplet (τ_0 = 16 μs), one might still expect the majority of the chemistry to occur form the triplet manifold. However, this is ultimately dependent on the rate at which the different components of the system quench the excited states of the photocatalyst and on the concentrations employed. To determine these rates, we have employed a combination of steady-state/time-resolved fluorescence and laser flash photolysis techniques.

To determine the singlet quenching values, we have performed steady-state fluorescence quenching studies. By monitoring the quenching of α-6T fluorescence emission as a function of quencher concentration [Q] (Figure 1) and employing the Stern−Volmer analysis of eq 2:[25,26]

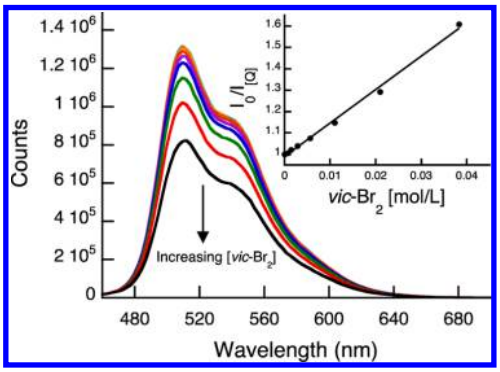

Figure 1. Kinetic analysis of the reaction between $^1\alpha$-6T and *vic*-Br_2. Steady-state fluorescence spectrum of α-6T (λ_{ex} = 450 nm) in the presence of increasing concentrations of *vic*-Br_2. Inset shows a Stern−Volmer plot displaying the decrease in fluorescence intensity, as a function of *vic*-Br_2 concentration.

$$\frac{I_0}{I_{[Q]}} = 1 + K_{SV}[Q] \quad (2)$$

where I_0 and I are the fluorescence intensities in the absence and in the presence of quencher; [Q] is the concentration of quencher; and K_{SV} is the Stern−Volmer constant. From the slope of the linear Stern−Volmer quenching plot (Figure 1, inset), one can obtain the corresponding K_{SV} value. For example, from the data shown in Figure 1, we find that K_{SV} for the model *vic*-Br_2 is 15.6 M^{-1}. However, for dynamic quenching, K_{SV} is given by eq 2:

$$K_{SV} = k_q\tau_0 \quad (3)$$

where k_q is the quenching rate constant and τ_0 is the fluorescence lifetime of α-6T in the absence of quencher, a value of $k_q = 1.93 \times 10^{10}$ M^{-1} s^{-1} can be calculated for the *vic*-Br_2. Using this technique, we have also determined k_q for other components of the system, which may compete for $^1\alpha$-6T (see Table 4).

Table 4. Singlet Quenching of α-Sexithiophene

entry	quencher [Q]	K_{SV} (M^{-1})[a]	k_q (M^{-1} s^{-1})[b]
1	*vic*-Br_2	15.6	1.93×10^{10}
2	TMEDA	0.14	1.69×10^{8}
3	alkene	6.9	8.5×10^{9}

[a]Determined from the slope of the corresponding Stern−Volmer plot ($I_0/I_{[Q]}$ vs [Q]). [b]Based on a fluorescence lifetime of τ_0 = 0.81 ns.

From the data listed in Table 4, it can be seen that both the *vic*-Br_2 starting material and alkene product are efficient quenchers of $^1\alpha$-6T, with bimolecular rate constants at or approaching the diffusion control limit. In comparison, TMEDA was found to react with $^1\alpha$-6T at a rate roughly 2 orders of magnitude slower than that of the *vic*-Br_2 starting material. From this data, we were able to calculate that even with such a short lifetime, 49% of α-6T singlets are intercepted by the *vic*-Br_2 under initial reaction conditions using eq 4:

dx.doi.org/10.1021/cs501030f | ACS Catal. 2014, 4, 4034−4039

$$\text{percentage of } {}^1\alpha\text{-6T quenched by } \textit{vic}\text{-Br}_2 = \frac{100 \times k_q^{\textit{vic}\text{-Br}_2}[\textit{vic}\text{-Br}_2]}{\tau_0^{-1} + k_q^{\textit{vic}\text{-Br}_2}[\textit{vic}\text{-Br}_2] + k_q^{\text{amine}}[\text{amine}]} \quad (4)$$

With such a high percentage of singlets reacting with the *vic*-Br_2, it is likely that eT from $^1\alpha$-6T is playing a key role in our photocatalytic system. The fact that we also obtain 68% conversion (Table 1, entry 5) in the presence of O_2, a potent triplet quencher (k_q $^3\alpha$-6T = 3.0×10^9 M^{-1} s^{-1}), is also in good agreement with our rationalization of the singlet quenching data. However, since we obtain a >99% conversion (Table 1, entry 4) simply by purging the system of O_2, it may be a combination of both singlet and triplet eT that is responsible for part of the efficiency of our system, with the $^3\alpha$-6T capable of reducing any *vic*-Br_2 that escapes reaction with the singlet. To test this idea, we have performed time-resolved transient absorption spectroscopy on α-6T, using a nanosecond laser flash photolysis (LFP) system, with the objective of determining the rate at which the different components of the system quench the α-6T triplet. Figure 2 shows the data

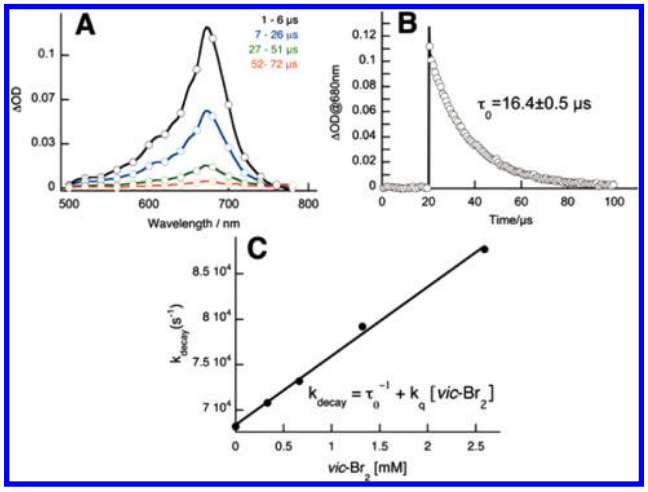

Figure 2. Kinetic analysis of the reaction between $^3\alpha$-6T and *vic*-Br_2: (A) transient spectrum showing the $^3\alpha$-6T signal at 680 nm obtained upon laser pulse excitation (355 nm, 10 mJ) of a α-6T sample which had been purged of oxygen, (B) the corresponding decay trace of $^3\alpha$-6T at 680 nm, and (C) kinetic quenching plot showing the rate of $^3\alpha$-6T quenching as a function of [*vic*-Br_2]. The slope of this plot corresponds to the bimolecular rate constant for this reaction (see the SI for experimental details).

from a typical quenching experiment used to determine the rate at which a *vic*-Br_2 reacts with $^3\alpha$-6T.These techniques were also applied to all other quenchers. The strong absorption (Figure 2A) and long lifetime (Figure 2B) of $^3\alpha$-6T greatly simplify these measurements.

As can be seen in Table 5, O_2 is the only component that efficiently quenches the triplet of α-6T. The *vic*-Br_2 and its corresponding alkene react at rates of ~10^6 M^{-1} s^{-1}, while the addition of TMEDA did not affect the rate of triplet decay.

With these data on hand, we are able to calculate, under initial reaction conditions, the percentage of triplets quenched by the *vic*-Br_2 in the presence and absence of O_2 using eq 5:[27]

Table 5. Triplet Quenching of α-Sexithiophene

entry	quencher [Q]	k_q (M^{-1} s^{-1})[a]
1	*vic*-Br_2	7.6×10^6
2	TMEDA	$<5 \times 10^5$
3	alkene	5.5×10^6
4	O_2	3.0×10^9

[a]Determined from the slope of the corresponding kinetic quenching plot (k_{decay} vs [Q]). See Figure 2C and theSI.

$$\text{percentage of } {}^3\alpha\text{-6T quenched by } \textit{vic}\text{-Br}_2 = \frac{100 \times k_q^{\textit{vic}-\text{Br}_2}[\textit{vic}\text{-Br}_2]}{\tau_0^{-1} + k_q^{\textit{vic}\text{-Br}_2}[\textit{vic}\text{-Br}_2] + k_q^{\text{amine}}[\text{amine}] + k_q^{O_2}[O_2]} \quad (5)$$

Interestingly, we find that, in the presence of O_2, only 7% of triplets are quenched by *vic*-Br_2. However, upon removal of O_2 from the system, this number increases to 89%. These results are again in excellent agreement with the idea of a combination of singlet and triplet eT, as well as the results observed in Table 1, entries 4 and 5.

Another key step in our proposed mechanism which can influence the efficiency of our system is catalyst turnover (see Scheme 1). Upon oxidation of the excited photocatalyst, the radical cation of α-6T is formed. Although it has been previously observed that photochemical generation of oligothiophene radical cations can result in chain elongation through radical cation recombination,[28−30] the α-$6T^{+\bullet}$ appears to be quite stable (τ_0 = 6 μs, see the SI). Therefore, to regenerate the neutral photocatalyst, we have included in our system TMEDA as the sacrificial e^- donor. Exploiting the fact that the α-$6T^{+\bullet}$ has a strong absorption at 780 nm, we can also determine the rate of catalyst turnover in the presence of TMEDA. Although the α-$6T^{+\bullet}$ can be generated through laser excitation of α-6T in the presence of *vic*-Br_2, we have found substitution of the *vic*-Br_2 with MV^{2+} results in more-efficient production of the oxidized photocatalyst (Scheme 2). By monitoring the rate of decay of the signal at 780 nm in the presence of increasing concentrations of TMEDA, we have been able to determine that TMEDA turns over the catalyst at a rate of 5.7×10^8 M^{-1} s^{-1} (see SI for experimental details and analysis), justifying its selection as the sacrificial electron donor.

Scheme 2. Indirect Generation of the α-Sexithiophene Radical Cation and Subsequent Quenching by Amine[a]

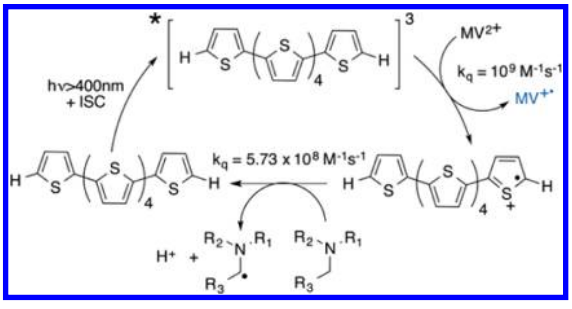

[a]Methyl viologen (MV^{2+}) is used as electron acceptor to generate α-$6T^{+\bullet}$ from $^3\alpha$-6T. $E^{red}_{1/2}(MV^{2+}/MV^{+\bullet})$ = −0.46 V vs SCE.[33] Quenching of α-$6T^{+\bullet}$ through e^- transfer from a tertiary amine results in the regeneration of the neutral photocatalyst and an α-amino radical after proton loss. $E^{ox}_{1/2}(R_3N/R_3N^{+\bullet})$ = 0.50 V vs SCE.[34]

dx.doi.org/10.1021/cs501030f | ACS Catal. 2014, 4, 4034−4039

Up to this point, we have been referring to TMEDA as solely a sacrificial e^- donor, whose role in the photocatalytic cycle is to simply turn the photocatalyst over from its oxidized state to a neutral state. However, recent publications from our group would suggest that this is most likely not the only role of TMEDA.[15,31] When tertiary aliphatic amines reductively quench a substrate under basic conditions, the resulting amine-radical cation will readily deprotonate to give an α-aminoalkyl radical, which, because of its reductive nature ($E^{ox}_{1/2}$ = −1.12 V vs SCE),[32] can, in turn, reduce a variety of organic substrates, including *vic*-dibromides.

Interested in examining the reactivity of the resulting TMEDA-derived α-aminoalkyl radicals with the model *vic*-Br_2 compound (Scheme 1), we set out to study this reaction utilizing LFP. However, since neither the α-aminoalkyl radical nor the product of its reaction with the *vic*-Br_2 give a signal in the attainable spectral region, we were required to use the probe technique.[35] It has been previously reported that (i) α-aminoalkyl radicals can be generated through reaction of the parent amine with *tert*-butoxyl radicals through H-abstraction and (ii) the resulting α-amino radicals are potent reducers of MV^{2+} (k_r = 10^9 M^{-1} s^{-1}).[36] Since *tert*-butoxyl radicals can be generated through direct photolysis of di-*tert*-butyl peroxide and reduced methyl viologen $MV^{+\bullet}$ has a strong absorption at 600 nm, the reduction of MV^{2+} would appear to be an ideal probe for our system, since any added *vic*-Br_2 would compete for the generated α-aminoalkyl radicals (Figures 3A and 3B).

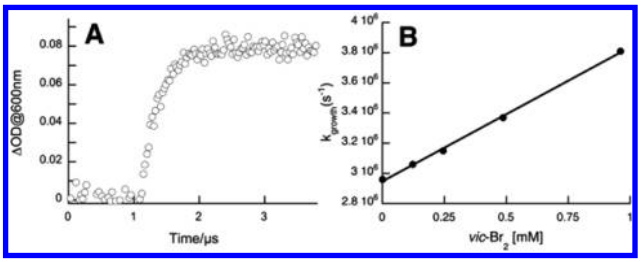

Figure 3. Kinetic analysis of the reaction between α-amino radicals of TMEDA and *vic*-Br_2 using the probe technique: (A) growth of reduced MV^{2+} at 600 nm in the absence of *vic*-Br_2 and (B) Stern−Volmer plot showing the rate of growth at 600 nm as a function of [*vic*-Br_2]. The slope of this plot corresponds to the bimolecular rate constant for this reaction. (See the SI for experimental details.)

When di-*tert*-butyl peroxide is photodecomposed in the presence of TMEDA, the MV^{2+} probe, and the model *vic*-Br_2, reactions 6−10 need to be taken into consideration:

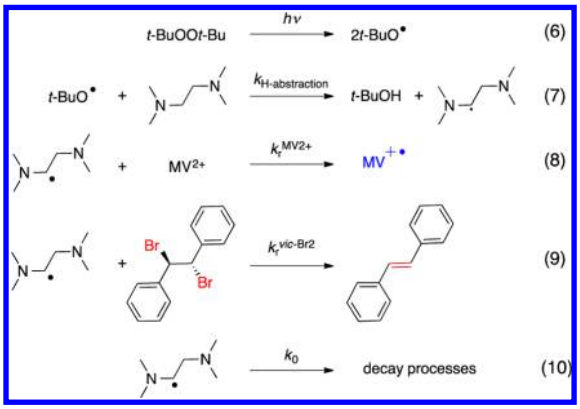

According to the mechanism described by reactions 6−10, the experimental pseudo-first-order rate constant (k_{growth}) for buildup of the $MV^{+\bullet}$ probe signal is given by eq 11:

$$k_{growth} = k_0 + k_r^{MV^{2+}}[MV^{2+}] + k_r^{vic\text{-}Br_2}[vic\text{-}Br_2] \quad (11)$$

The value of $k_r^{vic\text{-}Br_2}$ is thus obtained from the plot of k_{growth} versus the concentration of *vic*-Br_2, when the concentration of MV^{2+} is kept constant (Figure 3B). From this, we find that TMEDA-derived α-aminoalkyl radicals react with the model *vic*-Br_2 at a rate of 8.9×10^8 M^{-1} s^{-1}, which indirectly implies that some of the observed conversion may be due in part to reducing α-aminoalkyl radicals formed upon catalyst turnover. However, it should be mentioned that such a pathway is only likely to occur when the reaction is purged of O_2, as it is well-known that α-aminoalkyl radicals react quickly with O_2 to give α-aminoalkylperoxyl radicals ($k_r \approx 10^9$ M^{-1} s^{-1}).[37]

Lastly, it should be noted that catalyst turnover is only one of two possible routes to forming the α-aminoalkyl radical in our photocatalytic system. Previous reports have shown that $Br^\bullet$ radicals, liberated upon initial reduction of the *vic*-Br_2, can abstract a hydrogen from aliphatic amines at diffusion-controlled rates to generate the corresponding α-aminoalkyl radical (Scheme 3).[13,14] However, it is not until you combine

Scheme 3. Alternative Pathway for the Formation of α-Amino Radicals

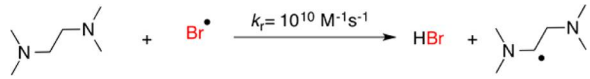

this route with the α-aminoalkyl radicals ability to reduce *vic*-Br_2 that it quickly becomes apparent that, depending on the reduction potential of the substrate, a chain reaction, as illustrated in Scheme 4, may be responsible for part of the

Scheme 4. Proposed Chain Reaction for the Dehalogenation of Vicinal Dibromides

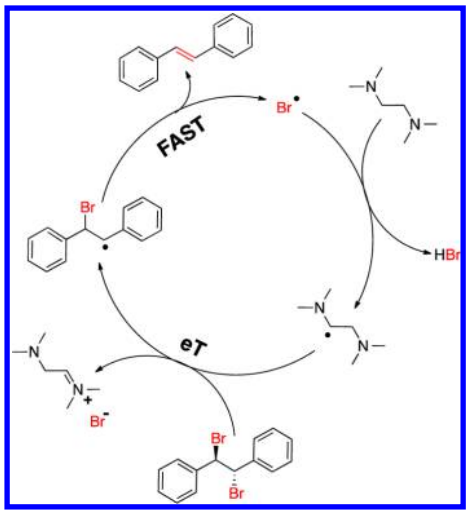

observed high conversion. In good agreement with this idea, we have found, under conditions of intermittent irradiation (see Figure S7 in the SI), that there is a nonlinear dependence between the rate of sample illumination and conversion, as would be expected for a chain reaction.

dx.doi.org/10.1021/cs501030f | ACS Catal. 2014, 4, 4034−4039

CONCLUSION

We have demonstrated, for the first time, the use of α-sexithiophene (α-6T) as a visible-light photoredox catalyst in the reductive dehalogention of *vic*-dibromides. The resulting photocatalytic system based on a combination of α-6T, tetramethylenediamine (TMEDA), and visible light has been demonstrated to reductively dehalogenate a variety of different *vic*-dibromides in good to excellent yield under relatively short irradiation times. Through examination of the thermodynamic feasibility and rate constants of the key mechanistic steps, we have been able to better understand the underlying mechanisms, which contribute to the high efficiency of our catalytic system.

ASSOCIATED CONTENT

Supporting Information

Details on reaction conditions, spectral data on products, conversion-versus-time plots, laser flash photolysis data, quenching plots, and NMR spectra. This material is available free of charge via the Internet at http://pubs.acs.org.

AUTHOR INFORMATION

Corresponding Author

*E-mail: scaiano@photo.chem.uottawa.ca.

Notes

The authors declare no competing financial interest.

ACKNOWLEDGMENTS

This work was supported by the Natural Sciences and Engineering Research Council of Canada, the Canadian Foundation for Innovation, and the Canada Research Chairs Program.

REFERENCES

(1) Wuts, P. G. M.; Greene, T. W. *Greene's Protective Groups on Organic Synthesis*, 4th Edition; John Wiley & Sons: Hoboken, NJ, 2007; pp 1−16.
(2) Totten, L. A.; Jans, U.; Roberts, A. L. *Environ. Sci. Technol.* **2001**, *35*, 2268−2274.
(3) Kuivila, H. G.; Menapace, L. W. *J. Org. Chem.* **1963**, *28*, 2165−2167.
(4) Schubert, W. M.; Rabinovitch, B. S.; Larson, N. R.; Sims, V. A. *J. Am. Chem. Soc.* **1952**, *74*, 4590−4592.
(5) Vijayashree, N.; Samuelson, A. G. *Tetrahedron Lett.* **1992**, *33*, 559−560.
(6) Casanova, J.; Rogers, H. R. *J. Org. Chem.* **1974**, *39*, 2408−2410.
(7) Willner, I.; Tsfania, T.; Eichen, Y. *J. Org. Chem.* **1990**, *55*, 2656−2662.
(8) Maji, T.; Karmakar, A.; Reiser, O. *J. Org. Chem.* **2010**, *76*, 736−739.
(9) Andrieux, C. P.; Le Gorande, A.; Savéant, J.-M. *J. Electroanal. Chem.* **1994**, *371*, 191−196.
(10) Vaze, A.; Rusling, J. F. *Langmuir* **2006**, *22*, 10788−10795.
(11) Bosser, G.; Paris, J. *J. Chem. Soc., Perkin Trans. 2* **1992**, 2057−2063.
(12) Lexa, D.; Saveant, J. M.; Schaefer, H. J.; Su Khac, B.; Vering, B.; Wang, D. L. *J. Am. Chem. Soc.* **1990**, *112*, 6162−6177.
(13) Scaiano, J. C.; Barra, M.; Krzywinski, M.; Sinta, R.; Calabrese, G. *J. Am. Chem. Soc.* **1993**, *115*, 8340−8344.
(14) Scaiano, J. C.; Barra, M.; Sinta, R. *Chem. Mater.* **1996**, *8*, 161−166.
(15) Pitre, S. P.; McTiernan, C. D.; Ismaili, H.; Scaiano, J. C. *J. Am. Chem. Soc.* **2013**, *135*, 13286−13289.
(16) Ravelli, D.; Fagnoni, M.; Albini, A. *Chem. Soc. Rev.* **2013**, *42*, 97−113.
(17) Nicewicz, D. A.; Nguyen, T. M. *ACS Catal.* **2014**, *4*, 355−360.
(18) Zhang, M.; Rouch, W. D.; McCulla, R. D. *Eur. J. Org. Chem.* **2012**, 6187−6196.
(19) Rouch, W. D.; Zhang, M.; McCulla, R. D. *Tetrahedron Lett.* **2012**, *53*, 4942−4945.
(20) Sakai, J.; Taima, T.; Yamanari, T.; Saito, K. *Sol. Energy Mater. Sol. Cells* **2009**, *93*, 1149−1153.
(21) Evans, C.; Weir, D.; Scaiano, J. C.; MacEachem, A.; Arnason, J. T.; Morand, P.; Hollebone, B.; Leitch, L. C.; Philogegne, B. J. R. *Photochem. Photobiol.* **1986**, *44*, 441−451.
(22) Janssen, R. A.; Moses, D.; Sariciftci, N. S. *J. Chem. Phys.* **1994**, *101*, 9519.
(23) *International Union of Pure and Applied Chemistry (IUPAC) Gold Book*, 2nd Edition; McNaught, A. D., Wilkinson, A., Eds.; Blackwell Science: Oxford, U.K., 1997.
(24) Oeter, D.; Egelhaaf, H.-J.; Ziegler, C.; Oelkrug, D.; Gopel, W. *J. Chem. Phys.* **1994**, *101*, 6344−6352.
(25) Lakowicz, J. R. *Principles of Fluorescence Spectroscopy*; Kluwer Academic−Plenum Publishers: New York, 1999; pp 278−330.
(26) Turro, N. J.; Ramamurthy, V.; Scaiano, J. C. *Modern Molecular Photochemistry of Organic Molecules*; University Science Publishers: New York, 2010; pp 1−483.
(27) James, H. J.; Broman, R. F. *Anal. Chim. Acta* **1969**, *48*, 411−417.
(28) Yagci, Y.; Jockusch, S.; Turro, N. J. *Macromolecules* **2007**, *40*, 4481−4485.
(29) Aydogan, B.; Yagci, Y.; Toppare, L.; Jockusch, S.; Turro, N. J. *Macromolecules* **2012**, *45*, 7829−7834.
(30) Fujitsuka, M.; Sato, T.; Segawa, H.; Shimidzu, T. *Synth. Met.* **1995**, *69*, 309−310.
(31) Ismaili, H.; Pitre, S. P.; Scaiano, J. C. *Catal. Sci. Technol.* **2013**, *3*, 935−937.
(32) Jonsson, M.; Wayner, D. D. M.; Lusztyk, J. *J. Phys. Chem.* **1996**, *100*, 17539−17543.
(33) Michaelis, L.; E.S, H. *J. Gen. Physiol.* **1933**, *16*, 859−873.
(34) Cherevatskaya, M.; Neumann, M.; Füldner, S.; Harlander, C.; Kümmel, S.; Dankesreiter, S.; Pfitzner, A.; Zeitler, K.; König, B. *Angew. Chem., Int. Ed.* **2012**, *51*, 4062−4066.
(35) Scaiano, J. C. In *Reactive Intermediate Chemistry*; Moss, R. A., Platz, M. S., Jones, M., Eds.; John Wiley & Sons: Hoboken, NJ, 2004; pp 847−871.
(36) Kim-Thuan, N.; Scaiano, J. C. *Int. J. Chem. Kinet.* **1984**, *16*, 371−377.
(37) Lalevée, J.; Graff, B.; Allonas, X.; Fouassier, J. P. *J. Phys. Chem. A* **2007**, *111*, 6991−6998.